Chemistry of Polynuclear Metal Complexes with Bridging Carbene or Carbyne Ligands. Part 96.[1] Reactions with Phospha-alkynes; Crystal Structures of $[WFe\{\mu\text{-}C(C_6H_4Me\text{-}4)PC(Bu^t)(CO)_5\}(\eta\text{-}C_5Me_5)]$ and $[MoFe\{\mu\text{-}C(C_6H_4Me\text{-}4)\text{-}C(Bu^t)P\}(\mu\text{-}CO)(CO)_3(PMe_3)(\eta\text{-}C_5H_5)]$*

Helen F. Dare, Judith A. K. Howard, Thomas P. Spaniol, F. Gordon A. Stone, and Jürgen Szameitat
Department of Inorganic Chemistry, The University, Bristol BS8 1TS

The electronically unsaturated dimetal compound $[WFe(\mu\text{-}CC_6H_4Me\text{-}4)(CO)_5(\eta\text{-}C_5Me_5)]$ reacts with the phospha-alkynes R′C≡P (R′ = Bu^t or Pr^i) in thf (tetrahydrofuran) below room temperature to give the complexes $[WFe\{\mu\text{-}C(C_6H_4Me\text{-}4)PC(R')\}(CO)_5(\eta\text{-}C_5Me_5)]$. The structure of the species with R′ = Bu^t has been determined by *X*-ray diffraction. The metal–metal bond [W–Fe 2.720(2) Å] is spanned by the bridging group such that all three atoms of the CPC chain are attached to the iron atom [Fe–CC_6H_4Me-4 2.11(2), Fe–CBu^t 2.14(1), and Fe–P 2.336(5) Å] but only the terminal carbons ligate the tungsten centre [W–CC_6H_4Me-4 2.18(2), W–CBu^t 2.22(1) Å]. The iron carries three CO groups, and the tungsten is co-ordinated by two CO ligands and the C_5Me_5 ring. Reactions between the phospha-alkynes and the dimetal compounds $[MFe(\mu\text{-}CC_6H_4Me\text{-}4)(CO)_4(PMe_3)(\eta\text{-}C_5H_5)]$ (M = Mo or W) in thf afford under mild conditions the complexes $[MFe\{\mu\text{-}C(C_6H_4Me\text{-}4)PC(R')\}(CO)_4(PMe_3)(\eta\text{-}C_5H_5)]$ (M = Mo, R′ = Bu^t or Pr^i; M = W, R′ = Bu^t), containing a similar bridge system. The two molybdenum–iron compounds readily isomerise in solution, yielding the species $[MoFe\{\mu\text{-}C(C_6H_4Me\text{-}4)C(R')P\}(\mu\text{-}CO)(CO)_3(PMe_3)(\eta\text{-}C_5H_5)]$. An *X*-ray diffraction study on one of the isomers (R′ = Bu^t) revealed an asymmetric unit containing two crystallographically independent molecules of similar geometry. The Mo(1)–Fe(1) bond [2.710(1) Å] is bridged by a carbonyl ligand and by the $C(C_6H_4Me\text{-}4)C(Bu^t)P$ unit. All these atoms of the CCP group are bonded to the molybdenum atom [Mo(1)–CC_6H_4Me-4 2.290(4), Mo(1)–CBu^t 2.353(5), and Mo(1)–P(1) 2.527(2) Å], but only the P and CC_6H_4Me-4 groups are attached to the iron [Fe(1)–CC_6H_4Me-4 2.017(5), Fe(1)–P(1) 2.302(2) Å]. The Mo atom carries the η-C_5H_5 ring and a CO ligand but the latter is bent [Mo(1)–C–O 168.4(4)°] towards the μ-P atom [C ··· P 2.380(5) Å]. The Fe atom is co-ordinated by two terminally bound CO groups and the PMe_3 ligand [Fe(1)–P(2) 2.246(2) Å]. The n.m.r. spectra (^1H, $^{13}C\text{-}\{^1H\}$, and $^{31}P\text{-}\{^1H\}$) of the new compounds are reported and discussed.

In this series of papers we have reported the synthesis of several dimetal compounds in which bonds between dissimilar transition elements are bridged by alkylidyne ligands. In general these groups are very reactive, and in studies on reactions of the dimetal compounds with substrate molecules we have identified many new C–H, C–C, and C–X (X = O, S, or Se) bond-forming processes.[2] Alkynes in particular afford a variety of complexes as a result of coupling with the alkylidyne groups.[3] The simplest products are those in which an alkyne molecule combines with a CR (R = alkyl or aryl) ligand to give a μ-C_3 bridged system [Scheme 1 (**A**)]. However, more complicated reactions have also been observed. Thus the C–C bond-forming step may be accompanied by a CO insertion process, or a hydrogen-atom migration if the alkyne has alkyl substituents.[3c–e]

It has recently become apparent that phospha-alkynes, in particular Bu^{t}C≡P, have an extensive co-ordination chemistry.[4,5] Since phospha-alkynes are isolobal with alkynes, we have studied reactions of the species R′C≡P (R′ = Bu^t or Pr^i) with some μ-alkylidyne dimetal compounds to establish whether coupling of alkylidyne and R′C≡P groups would occur at a dimetal centre in a manner analogous with that of alkynes (Scheme 1). However, if a similar reaction were to take place, formation of one or other, or a mixture, of two isomeric species (**B**) and (**C**) could result. A preliminary account of some of the results described herein has been given.[6]

Results and Discussion

Treatment of a thf (tetrahydrofuran) solution of the electronically unsaturated 32-valence-electron dimetal compound $[WFe(\mu\text{-}CC_6H_4Me\text{-}4)(CO)_5(\eta\text{-}C_5Me_5)]$ (**1**)[7] with Bu^{t}C≡P at *ca.* −5 °C afforded the dark green crystalline compound $[WFe\{\mu\text{-}C(C_6H_4Me\text{-}4)PC(Bu^t)\}(CO)_5(\eta\text{-}C_5Me_5)]$ (**2a**). A similar reaction between (**1**) and Pr^{i}C≡P gave the related complex $[WFe\{\mu\text{-}C(C_6H_4Me\text{-}4)PC(Pr^i)\}(CO)_5(\eta\text{-}C_5Me_5)]$ (**2b**). Data characterising these compounds are given in Tables 1 and 2. Both species displayed molecular ions in their mass spectra, but discussion of the other spectroscopic properties is deferred until the results of an *X*-ray diffraction study on (**2a**) have been described.

The molecular structure of (**2a**) is shown in Figure 1, and selected internuclear distances and angles are listed in Table 3. The metal–metal bond is spanned by the $C(C_6H_4Me\text{-}4)PC(Bu^t)$ fragment, with the C(1), P, and C(2) atoms attached to the iron

---

* 1,1,1,2,2-Pentacarbonyl-μ-[4′,4′-dimethyl-1′-*p*-tolyl-2′-phosphapent-1′-en-1′-yl-3′-ylidene-$C^{1',3'}$(Fe,W)*P*(Fe)]-2-(η-pentamethylcyclopentadienyl)irontungsten (*Fe–W*) and μ-carbonyl-1,1,2-tricarbonyl-2-(η-cyclopentadienyl)-μ-[2′-t-butyl-1′-*p*-tolyl-3′-phosphaprop-1′-en-1′-yl-3′-ylidene-C''(Fe,Mo)$C^{2'}$(Mo)*P*(Fe,Mo)]-1-(trimethylphosphine)ironmolybdenum (*Fe–Mo*).

Supplementary data available: see Instructions for Authors, *J. Chem. Soc., Dalton Trans.*, 1990, Issue 1, pp. xix—xxii.

Table 1. Analytical[a] and physical data for the dimetal complexes

Compound	Colour	Yield(%)	$\nu_{max.}(CO)^b/cm^{-1}$	Analysis(%) C	Analysis(%) H
(2a) $[WFe\{\mu\text{-}C(C_6H_4Me\text{-}4)PC(Bu^t)\}(CO)_5(\eta\text{-}C_5Me_5)]$	Green	52	2 040vs, 1 985s, 1 975vs, 1 911m	[c]46.9(46.8)	4.7(4.4)
(2b) $[WFe\{\mu\text{-}C(C_6H_4Me\text{-}4)PC(Pr^i)\}(CO)_5(\eta\text{-}C_5Me_5)]$	Green	66	2 040vs, 1 985s, 1 976vs, 1 916w	45.0(46.0)	4.5(4.2)
(5a) $[MoFe\{\mu\text{-}C(C_6H_4Me\text{-}4)PC(Bu^t)\}(CO)_4(PMe_3)(\eta\text{-}C_5H_5)]$	Brown	63	2 000vs, 1 950m, 1 941s	48.8(49.4)	5.2(5.0)
(5b) $[MoFe\{\mu\text{-}C(C_6H_4Me\text{-}4)PC(Pr^i)\}(CO)_4(PMe_3)(\eta\text{-}C_5H_5)]$	Red-brown	75	2 003vs, 1 957m, 1 941s	47.9(48.5)	5.0(4.8)
(5c) $[WFe\{\mu\text{-}C(C_6H_4Me\text{-}4)PC(Bu^t)\}(CO)_4(PMe_3)(\eta\text{-}C_5H_5)]$	Brown	49	1 996vs, 1 945m, 1 934vs	43.3(43.1)	4.4(4.3)
(6a) $[MoFe\{\mu\text{-}C(C_6H_4Me\text{-}4)C(Bu^t)P\}(\mu\text{-}CO)(CO)_3(PMe_3)(\eta\text{-}C_5H_5)]$	Red	30	[d]1 980vs, 1 925vs, 1 873s, 1 755m		
(6b) $[MoFe\{\mu\text{-}C(C_6H_4Me\text{-}4)C(Pr^i)P\}(\mu\text{-}CO)(CO)_3(PMe_3)(\eta\text{-}C_5H_5)]$	Red	56	[d]1 978vs, 1 920vs, 1 886s, 1 760m		

[a] Calculated values are given in parentheses. [b] In n-hexane, unless otherwise stated. [c] Crystallises with half a molecule of CH_2Cl_2. [d] In CH_2Cl_2.

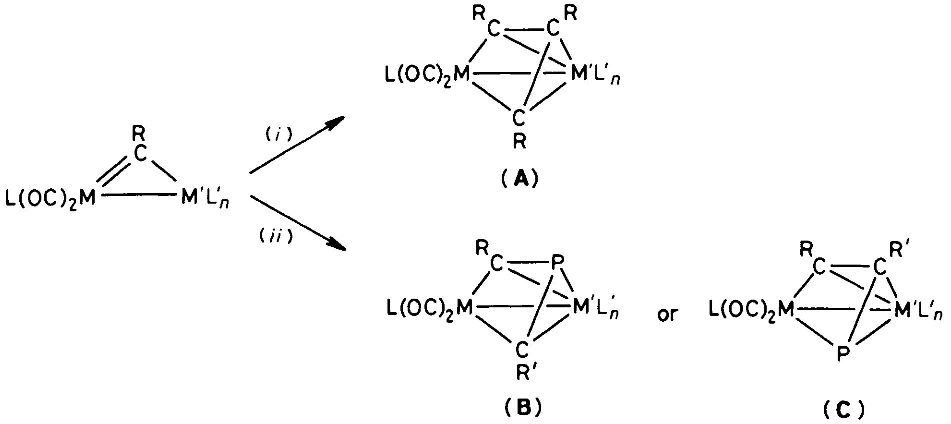

Scheme 1. L = η-C_5H_5 or η-C_5Me_5, R = alkyl or aryl, R' = Bu^t or Pr^i, M = Mo or W, $M'L'_n$ = metal-ligand group. (*i*) RC≡CR; (*ii*) R'C≡P

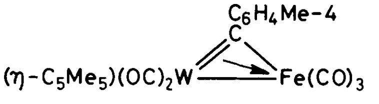

(1)

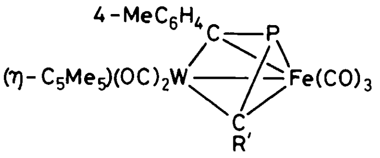

	R'
(2a)	Bu^t
(2b)	Pr^i

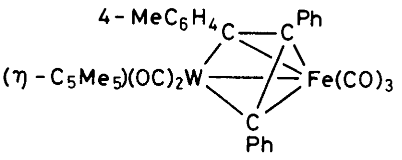

(3)

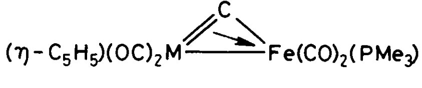

	M
(4a)	Mo
(4b)	W

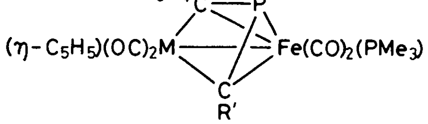

	M	R'
(5a)	Mo	Bu^t
(5b)	Mo	Pr^i
(5c)	W	Bu^t

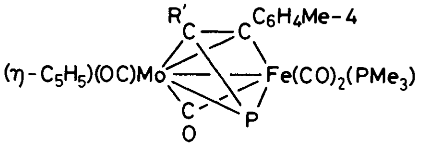

	R'
(6a)	Bu^t
(6b)	Pr^i

Table 2. Hydrogen-1, carbon-13, and phosphorus-31 n.m.r. data[a] for the complexes

Compound	^{1}H(δ)[b]	^{13}C(δ)[c]	^{31}P(δ)[b,d]
(2a)	1.11 (s, 9 H, Bu^t), 1.91 (s, 15 H, C_5Me_5), 2.21 (s, 3 H, Me-4), 6.98, 7.04 [$(AB)_2$, 4 H, C_6H_4, *J*(AB) 8]	222.9 [WCO, *J*(WC) 142], 219.8 [WCO, *J*(WC) 130], 214.3 (FeCO), 151.9 [d, μ-*C*Bu^t, *J*(PC) 62, *J*(WC) 55], 146.1 [d, $C^1(C_6H_4)$, *J*(PC) 12], 135.7, 128.4 (C_6H_4) 126.0 [d, $C^{2,6}(C_6H_4)$, *J*(PC) 15], 123.0 [d, μ-*C*C_6H_4Me-4, *J*(PC) 57, *J*(WC) 51], 101.4 (*C*$_5$Me$_5$), 44.7 [d, *C*Me$_3$, *J*(PC) 12], 36.3 [d, C*Me*$_3$, *J*(PC) 9], 21.1 (Me-4), 11.2 (C$_5$*Me*$_5$)	177.2(s)
(2b)	0.93 [d, 3 H, CH*Me*$_2$, *J*(HH) 7], 1.07 [d, 3 H, CH*Me*$_2$, *J*(HH) 7], 1.91 (s, 15 H, C_5Me_5), 2.22 (s, 3 H, Me-4), 2.55 (m, H, C*H*Me$_2$), 6.92, 7.05 [$(AB)_2$, 4 H, C_6H_4, *J*(AB) 8]	222.0 [WCO, *J*(WC) 140], 219.8 [WCO, *J*(WC) 134], 214.2 (FeCO), 150.5 [d, μ-*C*Pr^i, *J*(PC) 62, *J*(WC) 50], 146.0 [d, $C^1(C_6H_4)$, *J*(PC) 11], 135.8, 128.5 (C_6H_4), 126.2 [d, μ-*C*C_6H_4Me-4, *J*(PC) 56], 126.1 [d, $C^{2,6}(C_6H_4)$, *J*(PC) 16], 100.8 (*C*$_5$Me$_5$), 40.4 [d, *C*HMe$_2$, *J*(PC) 12], 27.8 [d, CH*Me*$_2$, *J*(PC) 6], 25.7 [d, CH*Me*$_2$, *J*(PC) 15], 21.1 (Me-4), 10.7 (C$_5$*Me*$_5$)	169.6(s)
(5a)[e]	1.26 (s, 9 H, Bu^t), 1.29 [d, 9 H, MeP, *J*(PH) 10], 2.22 (s, 3 H, Me-4), 5.03 (s, 5 H, C_5H_5), 6.92, 7.22 [$(AB)_2$, 4 H, C_6H_4, *J*(AB) 8]	[f]238.7, 237.1 (MoCO), 218.7 [d, FeCO, *J*(PC) 29], 216.5 [d, FeCO, *J*(PC) 21], 177.8 [d, μ-*C*Bu^t, *J*(PC) 63], 151.6 [d, $C^1(C_6H_4)$, *J*(PC) 11], 136.3 [d, μ-*C*C_6H_4Me-4, *J*(PC) 55], 134.4, 128.7 (C_6H_4), 125.9 [d, $C^{2,6}(C_6H_4)$, *J*(PC) 13], 91.0 (C_5H_5), 45.0 [d, *C*Me$_3$, *J*(PC) 11], 36.2 [d, C*Me*$_3$, *J*(PC) 7], 21.3 [d of d, MeP, *J*(PC) 34 and 4], 21.2 (Me-4)	185.9 [d μ-CPC, *J*(PP) 15], 30.9 [d, MeP, *J*(PP) 15]
(5b)	1.07 [d, 3 H, CH*Me*$_2$, *J*(HH) 7], 1.12 [d, 3 H, CH*Me*$_2$, *J*(HH) 7], 1.34 [d, 9 H, MeP, *J*(PH) 10], 2.22 (s, 3 H, Me-4), 3.09 (m, 1 H, C*H*Me$_2$), 4.97 (s, 5 H, C_5H_5), 6.92, 7.18 [$(AB)_2$, 4 H, *J*(AB) 8]	[g]238.1, 234.4 (MoCO), 218.6 [d, FeCO, *J*(PC) 29], 216.5 [d, FeCO, *J*(PC) 22], 168.9 [d, μ-*C*Pr^i, *J*(PC) 64], 151.2 [d, $C^1(C_6H_4)$, *J*(PC) 11], 137.2 [d, μ-*C*C_6H_4Me-4, *J*(PC) 53], 134.4, 128.7 (C_6H_4), 125.6 [d, $C^{2,6}(C_6H_4)$, *J*(PC) 13], 91.1 (C_5H_5), 42.9 [d, CH*Me*$_2$, *J*(PC) 9], 29.6 (CH*Me*$_2$), 26.6 [d, CH*Me*$_2$, *J*(PC) 15], 21.6 [d of d, MeP, *J*(PC) 35 and 4], 21.2 (Me-4)	182.4 [d, μ-CPC, *J*(PP) 12], 32.0 [d, MeP, *J*(PP) 12]
(5c)	1.19 (s, 9 H, Bu^t), 1.34 [d, 9 H, MeP, *J*(PH) 10], 2.19 (s, 3 H, Me-4), 5.13 (s, 5 H, C_5H_5), 6.89, 7.12 [$(AB)_2$, 4 H, C_6H_4, *J*(AB) 8]	225.2 [WCO, *J*(WC) 133], 225.0 [WCO, *J*(WC) 131], 218.9 [d, FeCO, *J*(PC) 30], 216.9 [d, FeCO, *J*(PC) 22], 153.8 [d, μ-*C*Bu^t, *J*(PC) 61, *J*(WC) 59], 152.0 [d, $C^1(C_6H_4)$, *J*(PC) 12], 134.0, 128.6 (C_6H_4), 125.9 [d, $C^{2,6}(C_6H_4)$, *J*(PC) 14], 112.8 [d, μ-*C*C_6H_4Me-4, *J*(PC) 52, *J*(WC) 54], 89.2 (C_5H_5), 44.9 [d, *C*Me$_3$, *J*(PC) 12], 35.9 [d, C*Me*$_3$, *J*(PC) 8], 21.6 [d of d, MeP, *J*(PC) 33 and 5], 21.0 (Me-4)	187.7 [d μ-CPC, *J*(PP), 15], 32.1 [d, MeP, *J*(PP) 15]
(6a)	1.09 (s, 9 H, Bu^t), 1.28 [d, 9 H, MeP, *J*(PH) 8], 2.27 (s, 3 H, Me-4), 5.29 (s, 5 H, C_5H_5), 6.99, 7.01 [$(AB)_2$, 4 H, C_6H_4, *J*(AB) 9]	264.0 (μ-CO), 242.0 [d, MoCO, *J*(PC) 40], 214.8 [d, FeCO, *J*(PC) 11], 210.9 [d of d, FeCO, *J*(PC) 7 and 7.5], 150.5 [d of d, μ-*C*Bu^t, *J*(PC) 71 and 12], 149.3 [$C^1(C_6H_4)$], 134.9 (μ-*C*C_6H_4Me-4 and C_6H_4), 128.4, 127.8 (C_6H_4), 93.3 (C_5H_5), 40.5 [d, *C*Me$_3$, *J*(PC) 9], 31.4 [d, C*Me*$_3$, *J*(PC) 4], 21.1 (Me-4), 17.9 [d, MeP, *J*(PC) 28]	292.1 [d, μ-P, *J*(PP) 7], 14.4 [d, MeP, *J*(PP) 7]
(6b)	0.74 [d, 3 H, CH*Me*$_2$, *J*(HH) 6], 1.32 [d, 9 H, MeP, *J*(PH) 9], 1.59 [d, 3 H, CH*Me*$_2$, *J*(HH) 6], 2.28 (s, 3 H, Me-4), 2.56 (m, 1 H, C*H*Me$_2$), 5.04 (s, 5 H, C_5H_5), 7.05, 7.13 [$(AB)_2$, 4 H, C_6H_4, *J*(AB) 8]	262.9 (μ-CO), 240.3 [d, MoCO, *J*(PC) 37], 214.0 [d, FeCO, *J*(PC) 10], 211.8 [d, FeCO, *J*(PC) 10], 146.9 [d of d, μ-*C*Pr^i, *J*(PC) 71 and 12], 146.9 [$C^1(C_6H_4)$], 136.1 (C_6H_4 and μ-*C*C_6H_4Me-4), 128.6, 128.5 (C_6H_4) 94.6 (C_5H_5), 34.7 [d, *C*HMe$_2$, *J*(PC) 7], 28.0 (s, CH*Me*$_2$), 22.1 [d, CH*Me*$_2$, *J*(PC) 7], 21.1 (Me-4), 18.6 [d, MeP, *J*(PC) 29]	[h]291.1 [d, μ-P, *J*(PP) 7], 15.4 [d, MeP, *J*(PP) 7]

[a] Chemical shifts (δ) in p.p.m., coupling constants in Hz. Measurements at room temperature, unless otherwise stated. [b] Measured in CD_2Cl_2. [c] Hydrogen-1 decoupled, to high frequency of $SiMe_4$, measured in CD_2Cl_2–CH_2Cl_2. [d] Hydrogen-1 decoupled, chemical shifts to high frequency of 85% H_3PO_4 (external) taken as positive. [e] Data taken from spectra showing presence of *ca.* 5% of **(6a)**. [f] Measured at −40 °C. [g] Measured at −30 °C. [h] Data taken from measurements on a mixture of **(5b)** and **(6b)**.

atom [C(1)–Fe 2.11(2), P–Fe 2.336(5), and C(2)–Fe 2.14(1) Å] and with C(1) and C(2) also bonded to the tungsten atom [C(1)–W 2.18(2), and C(2)–W 2.22(1) Å]. The W···P separation (3.046 Å) is non-bonding. The five CO groups are terminally bound to their respective metal centres, three to the iron and two to the tungsten, with the latter as expected carrying the η-C_5Me_5 ring.

Several complexes prepared by treating heteronuclear dimetal compounds with alkynes have structures similar to that of **(2a)**. Thus PhC≡CPh with **(1)** affords [WFe{μ-C(C_6H_4Me-4)C(Ph)C(Ph)}$(CO)_5$(η-C_5Me_5)] **(3)**.[3c] Although the crystal structure of the latter has not been established by *X*-ray diffraction, it is firmly based on the spectroscopic properties, and, moreover, that of the closely related species [WFe{μ-C(C_6H_4Me-4)C(Me)C(Me)}$(CO)_5$(η-C_5H_5)] has been determined.[3a] The W–Fe distance [2.720(1) Å] in the latter is the same as that found for **(2a)** (Table 3). Interestingly, the structure of **(2a)** is of type **(B)** (Scheme 1), resulting from a P–C bond-forming process, in preference to a C–C bond synthesis which would have led to the alternative structure of type **(C)**. There was no evidence in the synthesis of complexes **(2)** for the formation of isomers with phosphorus atoms at the end of the μ-C_2P chains.

Table 3. Selected internuclear distances (Å) and angles (°) for $[WFe\{\mu\text{-}C(C_6H_4Me\text{-}4)PC(Bu^t)\}(CO)_5(\eta\text{-}C_5Me_5)]\cdot 0.5CH_2Cl_2$ (**2a**), with estimated standard deviations in parentheses

W–Fe	2.720(2)	W–C(1)	2.18(2)	W···P	3.046	W–C(2)	2.22(1)
W–C(6)	1.97(2)	W–C(7)	2.00(2)	Fe–P	2.336(5)	Fe–C(1)	2.11(2)
Fe–C(2)	2.14(1)	Fe–C(3)	1.77(2)	Fe–C(4)	1.75(2)	Fe–C(5)	1.76(2)
P–C(1)	1.76(2)	P–C(2)	1.77(1)	C(1)–C(11)	1.48(2)	C(2)–C(21)	1.54(2)
C(3)–O(3)	1.14(2)	C(4)–O(4)	1.15(2)	C(5)–O(5)	1.16(2)	C(6)–O(6)	1.17(2)
C(7)–O(7)	1.14(2)	W–C(C_5Me_5) (mean)	2.35				
Fe–W–C(1)	49.5(4)	Fe–W–C(2)	50.1(4)	C(1)–W–C(2)	67.9(5)	Fe–W–C(6)	81.4(5)
C(1)–W–C(6)	90.7(6)	C(2)–W–C(6)	130.1(6)	Fe–W–C(7)	84.9(5)	C(1)–W–C(7)	134.3(7)
C(2)–W–C(7)	85.8(6)	C(6)–W–C(7)	78.2(7)	W–Fe–P	73.6(1)	W–Fe–C(1)	51.8(4)
P–Fe–C(1)	46.4(4)	W–Fe–C(2)	52.8(4)	P–Fe–C(2)	46.4(4)	C(1)–Fe–C(2)	70.7(5)
W–Fe–C(3)	104.2(6)	P–Fe–C(3)	132.7(6)	C(1)–Fe–C(3)	155.9(7)	C(2)–Fe–C(3)	93.6(7)
W–Fe–C(4)	153.3(6)	P–Fe–C(4)	79.6(6)	C(1)–Fe–C(4)	108.4(7)	C(2)–Fe–C(4)	107.0(7)
C(3)–Fe–C(4)	93.5(8)	W–Fe–C(5)	101.7(6)	P–Fe–C(5)	131.5(6)	C(2)–Fe–C(5)	154.4(7)
C(3)–Fe–C(5)	95.6(8)	C(4)–Fe–C(5)	96.2(8)	Fe–P–C(1)	60.1(5)	Fe–P–C(2)	60.9(5)
C(1)–P–C(2)	88.2(7)	W–C(1)–P	100.7(7)	Fe–C(1)–P	73.6(6)	W–C(1)–C(11)	136(1)
Fe–C(1)–C(11)	121(1)	P–C(1)–C(11)	122(1)	W–C(2)–Fe	77.1(4)	W–C(2)–P	98.6(6)
Fe–C(2)–P	72.6(5)	W–C(2)–C(21)	138(1)	Fe–C(2)–C(21)	125(1)	P–C(2)–C(21)	121(1)
Fe–C(3)–O(3)	176(2)	Fe–C(4)–O(4)	176(2)	Fe–C(5)–O(5)	178(2)	W–C(6)–O(6)	173(1)
W–C(7)–O(7)	172(1)						

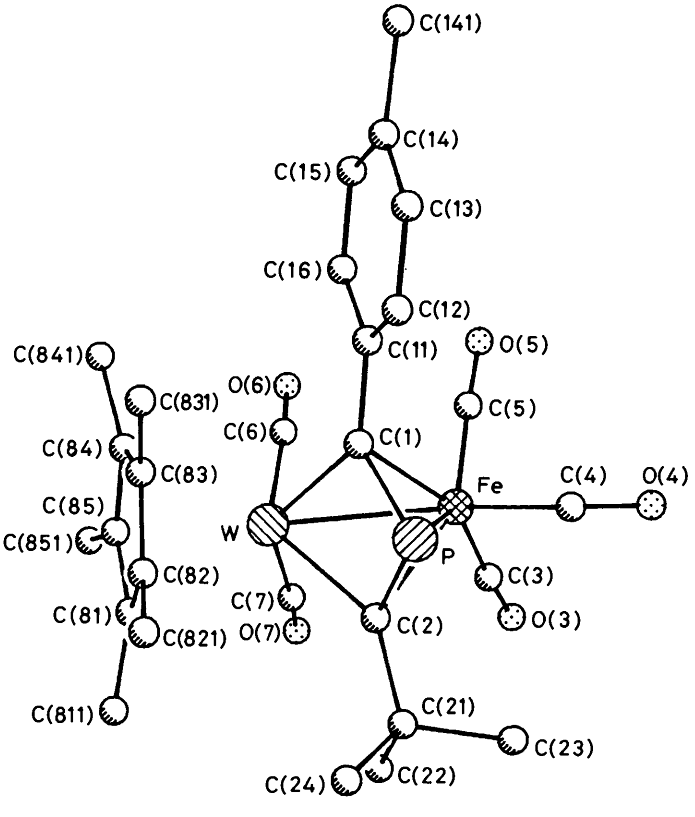

Figure 1. The molecular structure of $[WFe\{\mu\text{-}C(C_6H_4Me\text{-}4)PC(Bu^t)\}(CO)_5(\eta\text{-}C_5Me_5)]\cdot 0.5CH_2Cl_2$ (**2a**) showing the crystallographic atom labelling

Isolobal mapping[8] of a P atom with an alkylidyne or $W(CO)_2(\eta\text{-}C_5Me_5)$ group allows the compounds (**2**) and (**3**) to be related as 'cyclobutadiene' type complexes of $Fe(CO)_3$ fragments [Scheme 2(*a*)]. However, the cyclobutadiene ligand analogy should not be overstressed since the presence of the large W atoms in the compounds (**2**), or in complexes of type (**3**), distorts the four-membered rings away from planarity. In (**2a**) the W atom is displaced by 0.65 Å from the plane defined by C(1), C(2), and P. A similar displacement of the W atom occurs in $[WFe\{\mu\text{-}C(C_6H_4Me\text{-}4)C(Me)C(Me)\}(CO)_5(\eta\text{-}C_5H_5)]$.[3a] Consequently, an η^3-bonding mode of the ligated CPC and C_3 fragments, as depicted in Scheme 2(*b*), is perhaps a more correct way of viewing these molecules. The close similarity of the P–C(1) and P–C(2) distances in (**2a**) (Table 3) are in agreement with delocalisation in the μ-CPC fragment.

The n.m.r. data for the compounds (**2**) are in complete accord with the structure established for (**2a**) in the solid state. In the $^{13}C\text{-}\{^1H\}$ n.m.r. spectra of both species (Table 2) three resonances are seen in the CO region. Two of these signals show $^{183}W\text{-}^{13}C$ couplings, and thus can be assigned to the non-equivalent carbonyl ligands of the $W(CO)_2$ moiety. The remaining CO peak (δ *ca.* 214 p.p.m.), three times as intense as the others, is due to the $Fe(CO)_3$ group, with site exchange of the carbonyl ligands on the n.m.r. time-scale resulting in the appearance of one resonance. The signals for the ligated carbon atoms of the μ-*C*(C_6H_4Me-4)P*C*(R′) (R′ = Bu^t or Pr^i) moieties appear as doublets due to $^{31}P\text{-}^{13}C$ coupling. Moreover, $^{183}W\text{-}^{13}C$ satellite peaks are also observed. For (**2a**) these resonances occur at δ 151.9 and 123.0 p.p.m., and are assigned to the μ-*C*Bu^t and μ-*C*C_6H_4Me-4 nuclei, respectively. In a coupled ^{13}C n.m.r. spectrum the doublet resonance at 123.0 p.p.m. remained sharp, whereas that at 151.9 p.p.m. became broad due to coupling with the protons of the Bu^t group. Other peaks in the $^{13}C\text{-}\{^1H\}$ n.m.r. spectra of the compounds (**2**) may be attributed to the C_6H_4Me-4, C_5Me_5, and Bu^t or Pr^i groups. The $^{31}P\text{-}\{^1H\}$ n.m.r. spectra consist of singlet signals at δ 177.2 (**2a**) and 169.6 p.p.m. (**2b**), respectively. The absence of $^{183}W\text{-}^{31}P$ coupling on these resonances is in agreement with there being no W–P bond in these molecules. The ^1H n.m.r. spectra show the expected peaks.

The reaction between $Bu^tC{\equiv}P$ and the dimetal compound $[MoFe(\mu\text{-}CC_6H_4Me\text{-}4)(CO)_6(\eta\text{-}C_5H_5)]$ was next investigated but a complicated mixture of products was obtained, all formed in poor yield. In an attempt to obtain fewer products in reactions, with the phospha-alkynes, the electronically unsaturated molybdenum–iron complex $[MoFe(\mu\text{-}CC_6H_4Me\text{-}4)(CO)_4(PMe_3)(\eta\text{-}C_5H_5)]$ (**4a**)[10] was employed as a precursor. As described below, this approach was successful, and so studies were extended to include the tungsten-containing analogue $[WFe(\mu\text{-}CC_6H_4Me\text{-}4)(CO)_4(PMe_3)(\eta\text{-}C_5H_5)]$ (**4b**).

Treatment of the compound (**4a**) with $Bu^tC{\equiv}P$ in thf solutions at low temperatures (*ca.* 0 °C) afforded the complex [MoFe{μ-C-

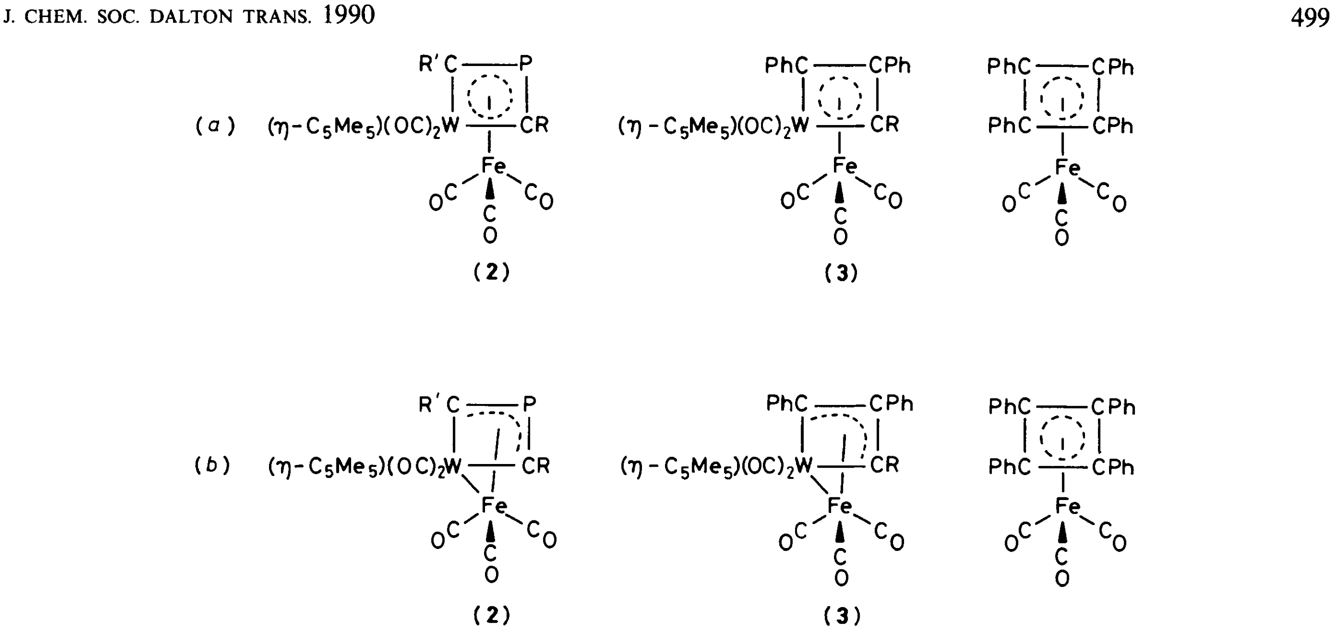

Scheme 2. R = C_6H_4Me-4, R′ = Bu^t or Pr^i

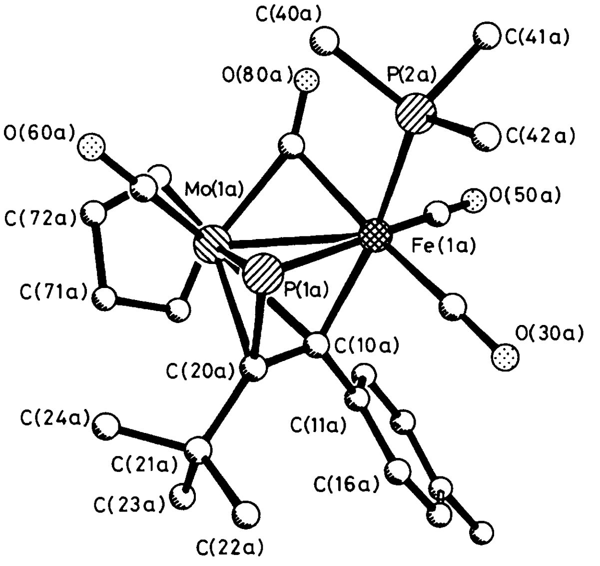

Figure 2. The molecular structure of one of the two chemically identical but crystallographically independent molecules of [MoFe{μ-C(C_6H_4-Me-4)C(Bu^t)P}(μ-CO)$(CO)_3(PMe_3)$(η-C_5H_5)] (**6a**) showing the atom labelling

(C_6H_4Me-4)PC(Bu^t)}$(CO)_4(PMe_3)$(η-C_5H_5)] (**5a**) as the major product, together with a small amount of its isomer [MoFe{μ-C(C_6H_4Me-4)C(Bu^t)P}(μ-CO)$(CO)_3(PMe_3)$(η-C_5H_5)] (**6a**), discussed further below. A similar reaction between Pr^{i}C≡P and (**4a**) yielded the compound [MoFe{μ-C(C_6H_4Me-4)PC(Pr^i)}-$(CO)_4(PMe_3)$(η-C_5H_5)] (**5b**). The reaction between the tungsten–iron compound (**4b**) and Bu^{t}C≡P proceeded more slowly at room temperature to give the complex [WFe{μ-C(C_6H_4Me-4)PC(Bu^t)}$(CO)_4(PMe_3)$(η-C_5H_5)] (**5c**). Data for the compounds (**5**) are listed in Tables 1 and 2.

The n.m.r. spectra for the complexes (**5**) indicate that these species contain μ-C(C_6H_4Me-4)PC(R′) groups as found in the compounds (**2**). Thus, as in the ^{13}C-{^{1}H} n.m.r. spectra of the latter, diagnostic signals are observed for the μ-*C*(C_6H_4Me-4)P*C*(R′) nuclei. For (**5b**) these are seen as doublets at δ 168.9 (μ-*C*Pr^i) and 137.2 p.p.m. (μ-*C*C_6H_4Me-4) with ^{31}P–^{13}C couplings of 64 and 53 Hz, respectively. Moreover, in a fully coupled ^{13}C spectrum, whereas the doublet at 137.2 p.p.m. remained sharp, that at δ 168.9 p.p.m. became broad, due to ^{1}H–^{13}C coupling with the protons of the isopropyl group. The ^{13}C-{^{1}H} spectrum shows four CO resonances at δ 238.1, 234.4 (MoCO), 218.6, and 216.5 p.p.m. (FeCO). The signals at 218.6 and 216.5 p.p.m. are doublets and therefore may be assigned to the carbonyls of the Fe$(CO)_2(PMe_3)$ group. The expected resonances appear in the ^{1}H n.m.r. spectrum. As with compound (**2b**), the Me groups of the Pr^i group are non-equivalent, a feature also discernible in the ^{13}C-{^{1}H} n.m.r. spectra. The ^{31}P-{^{1}H} n.m.r. spectrum of (**5b**) shows two doublet resonances [*J*(PP) 12 Hz] at δ 182.4 and 32.0 p.p.m. The latter is characteristic for a Fe$(CO)_2(PMe_3)$ group,[3e,10] and the former may be assigned on the basis of the chemical shift to the P nucleus in the bridging ligand.

The n.m.r. spectra (^{1}H, ^{13}C-{^{1}H}, and ^{31}P-{^{1}H}) of complexes (**5a**) and (**5c**) show similar features to those of (**5b**). However, measurements on samples of (**5a**) always revealed the presence of small amounts of the rearrangement product (**6a**). In contrast, when freshly prepared, compound (**5b**) does not show n.m.r. resonances due to its isomer [MoFe{μ-C(C_6H_4Me-4)C-(Pr^i)P}(μ-CO)$(CO)_3(PMe_3)$(η-C_5H_5)] (**6b**), discussed below.

Compound (**5a**) in CH_2Cl_2 solution at room temperature isomerises slowly to give (**6a**), forming the latter in yields of *ca.* 30% over a period of *ca.* 5 d. The two isomers may be separated by column chromatography at low temperatures, as described in the Experimental section. Compound (**5b**) does not isomerise in solution at room temperature, but on refluxing diethyl ether solutions for *ca.* 2 d there is a partial conversion into (**6b**), accompanied by some decomposition. In contrast, the tungsten–iron complex (**5c**) does not isomerise under the same conditions.

The spectroscopic data for the compounds (**6**) did not fully establish the structure of these species. Fortunately, suitable crystals of (**6a**) could be grown for an *X*-ray diffraction study. The asymmetric unit contains two structurally similar but crystallographically independent molecules. Data for one molecule are listed in Table 4, and the structure is shown in Figure 2.

The Mo(1)–Fe(1) bond [2.710(1) Å] is bridged both by a C(C_6H_4Me-4)C(Bu^t)P group and a carbonyl ligand [Fe(1)–C(80)–O(80) 129.7(3) and Mo(1)–C(80)–O(80) 148.6(4)°]. This μ-CO group is evidently responsible for the band in the i.r. spectrum of (**6a**) at 1 755 cm^{-1}. The C(C_6H_4Me-4)C(Bu^t)P

Table 4. Selected internuclear separations (Å) and angles (°) for $[MoFe\{\mu\text{-}C(C_6H_4Me\text{-}4)C(Bu^t)P\}(\mu\text{-}CO)(CO)_3(PMe_3)(\eta\text{-}C_5H_5)]$ (**6a**) (one of two independent molecules*) with estimated standard deviations in parentheses

Mo(1)–Fe(1)	2.710(1)	Mo(1)–P(1)	2.527(2)	Mo(1)–C(10)	2.290(4)	Mo(1)–C(20)	2.353(5)
Mo(1)–C(60)	1.963(5)	Mo(1)–C(70)	2.320(5)	Mo(1)–C(80)	2.003(5)	Fe(1)–P(1)	2.302(2)
Fe(1)–P(2)	2.246(2)	Fe(1)–C(10)	2.017(5)	Fe(1)–C(30)	1.755(5)	Fe(1)–C(50)	1.787(5)
Fe(1)–C(80)	2.159(5)	P(1)–C(20)	1.791(5)	P(1) ··· C(60)	2.380(5)	C(30)–O(30)	1.145(7)
C(50)–O(50)	1.144(6)	C(60)–O(60)	1.156(6)	C(80)–O(80)	1.180(6)	C(10)–C(11)	1.491(6)
C(10)–C(20)	1.406(6)	C(20)–C(21)	1.528(7)				

Fe(1)–Mo(1)–P(1)	52.0(1)	Fe(1)–Mo(1)–C(10)	46.6(1)	P(1)–Mo(1)–C(10)	61.7(1)
Fe(1)–Mo(1)–C(20)	65.4(1)	P(1)–Mo(1)–C(20)	42.9(1)	C(10)–Mo(1)–C(20)	35.2(1)
Fe(1)–Mo(1)–C(60)	101.1(1)	P(1)–Mo(1)–C(60)	62.5(1)	C(10)–Mo(1)–C(60)	123.6(2)
C(20)–Mo(1)–C(60)	94.3(2)	Fe(1)–Mo(1)–C(70)	124.8(1)	P(1)–Mo(1)–C(70)	142.1(1)
C(10)–Mo(1)–C(70)	89.5(2)	C(20)–Mo(1)–C(70)	99.3(2)	C(60)–Mo(1)–C(70)	133.7(2)
Fe(1)–Mo(1)–C(80)	51.9(1)	P(1)–Mo(1)–C(80)	87.9(1)	C(10)–Mo(1)–C(80)	94.6(1)
C(20)–Mo(1)–C(80)	116.9(2)	C(60)–Mo(1)–C(80)	90.8(2)	C(70)–Mo(1)–C(80)	120.5(2)
Mo(1)–Fe(1)–P(1)	59.9(1)	Mo(1)–Fe(1)–P(2)	117.2(1)	P(1)–Fe(1)–P(2)	90.9(1)
Mo(1)–Fe(1)–C(10)	55.6(1)	P(1)–Fe(1)–C(10)	69.1(1)	P(2)–Fe(1)–C(10)	160.4(1)
Mo(1)–Fe(1)–C(30)	136.6(2)	P(1)–Fe(1)–C(30)	91.6(2)	P(2)–Fe(1)–C(30)	93.2(2)
C(10)–Fe(1)–C(30)	85.2(2)	Mo(1)–Fe(1)–C(50)	107.9(2)	P(1)–Fe(1)–C(50)	167.3(2)
P(2)–Fe(1)–C(50)	98.6(2)	C(10)–Fe(1)–C(50)	101.0(2)	C(30)–Fe(1)–C(50)	96.3(2)
Mo(1)–Fe(1)–C(80)	46.9(1)	P(1)–Fe(1)–C(80)	90.4(1)	P(2)–Fe(1)–C(80)	83.8(1)
C(10)–Fe(1)–C(80)	98.4(2)	C(30)–Fe(1)–C(80)	176.4(2)	C(50)–Fe(1)–C(80)	82.3(2)
Mo(1)–P(1)–C(20)	63.4(1)	Fe(1)–P(1)–C(20)	83.6(1)	Mo(1)–P(1)–C(60)	47.1(1)
Fe(1)–P(1)–C(60)	102.0(1)	C(20)–P(1)–C(60)	98.2(2)	Mo(1)–C(10)–Fe(1)	77.7(2)
Mo(1)–C(10)–C(11)	132.1(3)	Fe(1)–C(10)–C(11)	120.9(3)	Mo(1)–C(10)–C(20)	74.9(2)
Fe(1)–C(10)–C(20)	105.7(3)	C(11)–C(10)–C(20)	128.7(4)	Mo(1)–C(20)–P(1)	73.7(2)
Mo(1)–C(20)–C(10)	69.9(3)	P(1)–C(20)–C(10)	100.9(3)	Mo(1)–C(20)–C(21)	126.0(3)
P(1)–C(20)–C(21)	124.3(3)	C(10)–C(20)–C(21)	134.1(4)	Fe(1)–C(30)–O(30)	177.8(5)
Fe(1)–C(50)–O(50)	179.1(4)	Mo(1)–C(60)–P(1)	70.4(2)	Mo(1)–C(60)–O(60)	168.4(4)
P(1)–C(60)–O(60)	121.1(3)	Mo(1)–C(70)–C(71)	73.4(3)	Mo(1)–C(80)–Fe(1)	81.2(2)
Mo(1)–C(80)–O(80)	148.6(4)	Fe(1)–C(80)–O(80)	129.7(3)		

* Data refer to molecule A of Table 6.

fragment spans the metal–metal bond such that the atoms P(1), C(20), and C(10) ligate the Mo centre [Mo(1)–P(1) 2.527(2), Mo(1)–C(10) 2.290(4), and Mo(1)–C(20) 2.353(5) Å], but only P(1) and C(10) are bonded to the Fe(1) atom [Fe(1)–P(1) 2.302(2), Fe(1)–C(10) 2.017(5), and Fe(1) ··· C(20) 2.75 Å]. The bridging unit is thus very different from that found in (**2a**). In (**6a**) the $C(C_6H_4Me\text{-}4)C(Bu^t)P$ group is η^3 co-ordinated to the molybdenum atom, which also carries the cyclopentadienyl ring and the C(60)O(60) ligand. However, the Mo(1)–C(60)–O(60) group is distinctly bent [168.4(4)°] towards P(1). This leads to a P(1) ··· C(60) [2.380(5) Å] interaction, discussed below. If the bridging C(80)O(80) ligand is ignored, the Mo atom has an η^4 attachment to the 1,2-ferraphosphacyclobutadiene ring C(10)FeP(1)C(20). Within this ring the P(1)–C(20) [1.791(5) Å] and C(10)–C(20) [1.406(6) Å] separations imply a degree of multiple-bond character. The iron atom is displaced by 0.14 Å from the plane defined by P(1)C(10)C(20). The two CO groups bonded to the iron atom have an essentially linear co-ordination mode, and the Me_3P ligand [Fe(1)–P(2) 2.246(2) Å] is transoid to the ligated carbon atom of the μ-CC_6H_4Me-4 fragment [P(2)–Fe(1)–C(10) 160.4(1)°].

Having established the structure of (**6a**) it became possible to interpret the n.m.r. data (Table 2) for this species, as well as those for (**6b**) which displays similar features. The $^{13}C\text{-}\{^1H\}$ n.m.r. spectrum of (**6a**) displays four CO resonances. The deshielded signal at δ 264.0 p.p.m. is diagnostic for a μ-CO ligand, as established by the crystal structure determination. The signal at δ 242.0 p.p.m. is a doublet [*J*(PC) 40 Hz] and must be due to the bent MoCO group, referred to above. The $^{31}P(1)\text{–}^{13}C(60)$ coupling is substantial, and we suggest that this is due to a donor bond resulting from transfer of the lone pair of electrons on the phosphorus atom into the π^* orbitals of the CO group. It is well established that the electron pair on a phosphorus atom incorporated into a delocalised ring system can bond to an atom external to the ring.[4,5] The remaining CO resonances at δ 214.8 and 210.9 p.p.m., are a doublet, and a doublet of doublets, respectively, and are due to the $Fe(CO)_2(PMe_3)$ group. The CO ligand showing coupling (*ca.* 7 Hz) to both ^{31}P nuclei is probably C(50) since it is transoid to P(1) [C(50)–Fe(1)–P(1) 167.3(2)°]. The μ-*C*Bu^t resonance appears as a doublet of doublets at δ 150.5 p.p.m. The larger $^{31}P\text{–}^{13}C$ coupling (71 Hz) is evidently due to the $^{31}P(1)\text{–}^{13}C(20)$ bond, with a three-bond coupling to P(2) being responsible for the smaller value (12 Hz). The resonance (134.9 p.p.m.) due to the $\mu\text{-}CC_6H_4Me\text{-}4$ nucleus is coincident with that for the C^4 peak of the C_6H_4 ring, and this signal is twice as intense as that for $C^1(C_6H_4)$ at δ 149.3 p.p.m. In accord with the structure established by *X*-ray diffraction, and in contrast with the spectrum of (**5a**), the resonances for the $\mu\text{-}CC_6H_4Me\text{-}4$ and $C^1(C_6H_4)$ nuclei show no $^{31}P\text{–}^{13}C$ coupling, appearing as singlets rather than doublets. Peaks in the ^1H n.m.r. spectrum are as expected. The $^{31}P\text{-}\{^1H\}$ n.m.r. spectrum shows doublet signals [*J*(PP) 7 Hz] at δ 292.1 and 14.4 p.p.m. The former resonance may be assigned to the ring phosphorus atom [P(1)] and the latter to the PMe_3 group, on the basis of the chemical shifts. The small value of the $^{31}P\text{–}^{31}P$ coupling reflects the cisoid P(2)–Fe(1)–P(1) [90.9(1)°] arrangement.

Possible pathways to the new compounds described above are shown in Scheme 3. Addition of a phospha-alkyne molecule to the electronically unsaturated iron centre in the compounds (**4**) could give intermediate (**I**), which could collapse to form the products (**5**). A similar pathway starting from the unsaturated complex (**1**) would yield the products (**2**). In principle, the η^2-ligated phospha-alkyne in (**I**) could

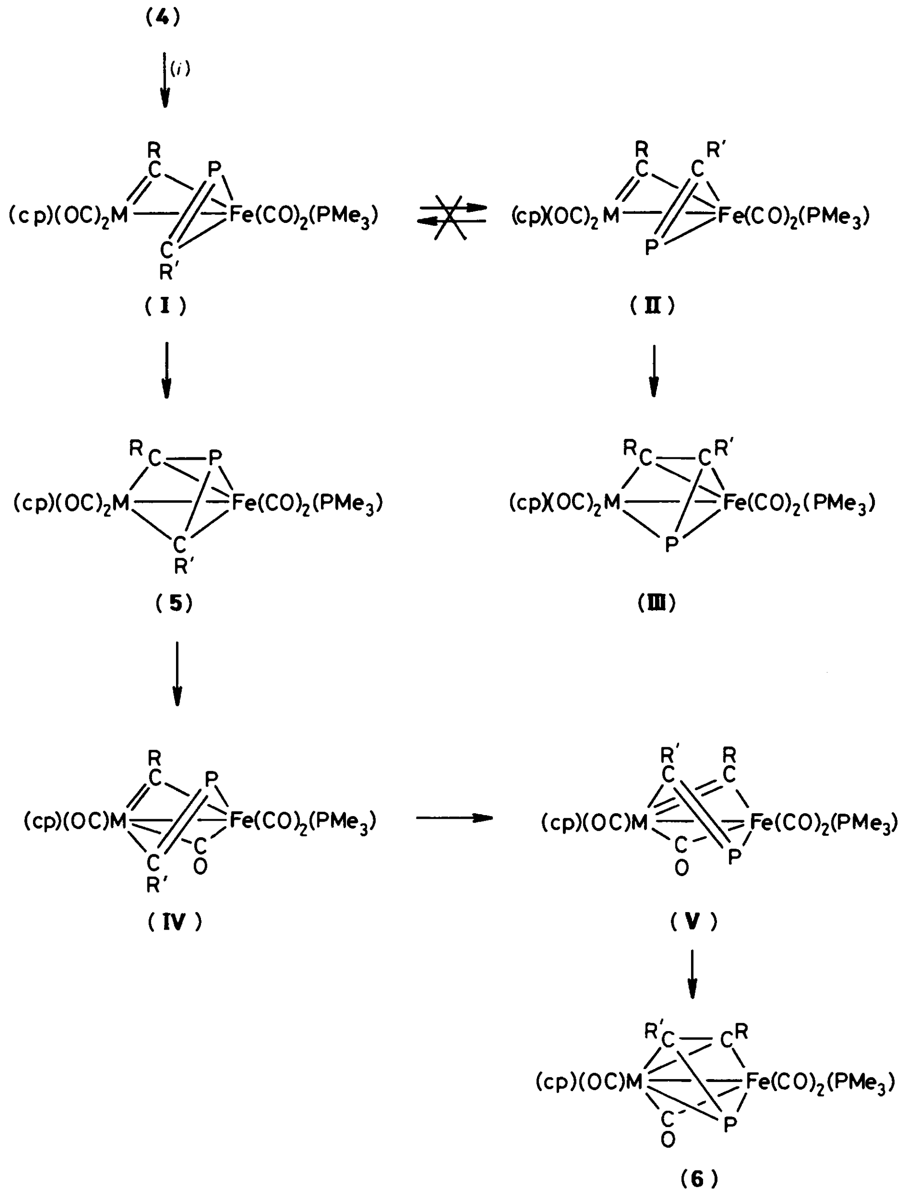

Scheme 3. cp = η-C_5H_5, R′ = Bu^t or Pr^i, R = C_6H_4Me-4, M = Mo or W. (*i*) + R′C≡P

rotate to give the intermediate (**II**) or the latter could form directly from (**4**). Collapse of (**II**) would then yield complexes with structure (**III**) [see (**C**) of Scheme 1]. Since no products of this nature were observed it appears that (**II**) is not an intermediate. Perhaps this is due to steric factors since its formation would place the bulky CR′ (R′ = Bu^t or Pr^i) and CC_6H_4Me-4 groups in (**II**) in close proximity at the iron centre.

The rearrangement of the molybdenum–iron compounds (**5a**) and (**5b**) into (**6a**) and (**6b**), respectively, could proceed *via* the intermediates (**IV**) and (**V**). This route involves cleavage of the P–CC_6H_4Me-4 bond, and migration of a CO group to a bridging position in (**IV**). Inversion of the MoFePCR ring in the latter could yield (**V**), which *via* C–C and Mo–P bond formation would give the compounds (**6**).

Irrespective of the mode of formation of the complexes (**2**), (**5**), and (**6**), we have demonstrated new P–C and C–C bond-forming processes at dimetal centres. Further studies with phospha-alkynes and other dimetal compounds with bridging alkylidyne or alkylidene ligands are clearly merited.

Experimental

Experiments were carried out using Schlenk-tube techniques, under a dry oxygen-free nitrogen atmosphere. All solvents were rigorously dried before use. Light petroleum refers to that fraction of b.p. 40—60 °C. Florisil (100—200 mesh) and Kieselgel (70—230 mesh) used for chromatography columns were obtained from Fluka. The compounds [WFe(μ-CC_6H_4Me-4)$(CO)_5$(η-C_5Me_5)],[7] [MFe(μ-CC_6H_4Me-4)-$(CO)_4(PMe_3)$(η-C_5H_5)] (M = Mo or W),[10,11] and R′C≡P (R′ = Bu^t [12] or Pr^i [13]) were prepared by methods previously described. The instrumentation used for the spectroscopic studies has been reported previously.[1] Analytical and other data for the new compounds are given in Table 1.

Reactions of the Phospha-alkynes with [WFe(μ-CC_6H_4Me-4)-$(CO)_5$(η-C_5Me_5)].—(*i*) A thf (20 cm^3) solution of complex (**1**) (0.21 g. 0.34 mmol) at −78 °C was treated with Bu^{t}C≡P (0.06 g, 0.60 mmol). The mixture was slowly warmed to *ca.* −5 °C and stirred magnetically for 10 min. Volatile material was removed

Table 5. Fractional atomic co-ordinates ($\times 10^4$) for complex (**2a**) with estimated standard deviations in parentheses

Atom	*x*	*y*	*z*
W	3 353(1)	6 855(1)	1 719(1)
Fe	5 424(2)	7 195(1)	903(1)
P	4 943(5)	5 851(3)	732(2)
C(1)	5 269(16)	6 234(9)	1 614(8)
C(11)	6 455(15)	5 967(9)	2 109(8)
C(12)	7 118(16)	5 272(10)	1 983(9)
C(13)	8 240(19)	4 990(10)	2 433(9)
C(14)	8 728(17)	5 416(11)	3 053(9)
C(141)	9 985(19)	5 108(13)	3 522(11)
C(15)	8 030(19)	6 089(10)	3 193(9)
C(16)	6 898(16)	6 351(9)	2 736(8)
C(2)	3 590(14)	6 546(8)	577(7)
C(21)	2 761(15)	6 602(9)	−161(8)
C(22)	1 805(17)	7 308(11)	−247(9)
C(23)	3 701(18)	6 638(10)	−781(8)
C(24)	1 871(18)	5 845(12)	−276(10)
C(3)	4 855(18)	8 053(10)	415(9)
O(3)	4 554(15)	8 622(8)	106(7)
C(4)	6 614(18)	6 949(11)	299(9)
O(4)	7 425(14)	6 833(10)	−93(7)
C(5)	6 589(19)	7 690(11)	1 529(9)
O(5)	7 391(12)	8 020(7)	1 922(7)
C(6)	4 330(16)	7 647(10)	2 360(8)
O(6)	4 782(12)	8 158(7)	2 742(6)
C(7)	2 528(20)	7 865(11)	1 323(9)
O(7)	2 026(16)	8 461(8)	1 176(7)
C(81)	1 128(17)	6 431(10)	1 842(9)
C(811)	−149(16)	6 612(13)	1 377(10)
C(82)	1 931(17)	5 728(10)	1 860(8)
C(821)	1 659(22)	4 997(10)	1 388(11)
C(83)	2 920(18)	5 745(10)	2 453(10)
C(831)	3 833(21)	5 054(14)	2 689(13)
C(84)	2 771(17)	6 428(12)	2 851(9)
C(841)	3 421(21)	6 655(13)	3 593(9)
C(85)	1 647(16)	6 870(12)	2 490(9)
C(851)	963(27)	7 632(14)	2 753(14)
Cl(1)	8 807(13)	8 636(7)	483(6)
Cl(2)	8 016(17)	10 174(8)	117(7)
C(9)	8 448(41)	9 434(25)	685(21)

in vacuo, and the residue was crystallised at −78 °C from toluene–hexane (*ca.* 4 $\mathrm{cm^3}$, 1:3) to afford dark green *crystals* of $[\mathrm{WFe}\{\mu\text{-}\mathrm{C(C_6H_4Me\text{-}4)PC(Bu^t)}\}(\mathrm{CO})_5(\eta\text{-}\mathrm{C_5Me_5})]$ (**2a**) (0.13 g).

(*ii*) In a similar experiment, a thf (20 $\mathrm{cm^3}$) solution of complex (**1**) (0.074 g, 0.12 mmol) was treated with an excess of $\mathrm{Pr^iC{\equiv}P}$ (*ca.* 0.24 mmol). After all volatile material had been removed *in vacuo* the residue was dissolved in $\mathrm{Et_2O}$ (2 $\mathrm{cm^3}$). Cooling to −78 °C yielded dark green *microcrystals* of $[\mathrm{WFe}\{\mu\text{-}\mathrm{C(C_6H_4\text{-}Me\text{-}4)PC(Pr^i)}\}(\mathrm{CO})_5(\eta\text{-}\mathrm{C_5Me_5})]$ (**2b**) (0.056 g), which were washed with light petroleum (2 × 1 $\mathrm{cm^3}$) at −78 °C.

Reactions of the Phospha-alkynes with the Compounds $[\mathrm{MFe}(\mu\text{-}\mathrm{CC_6H_4Me\text{-}4})(\mathrm{CO})_4(\mathrm{PMe_3})(\eta\text{-}\mathrm{C_5H_5})]$.—(*i*) A thf (25 $\mathrm{cm^3}$) solution of complex (**4a**) (0.165 g, 0.32 mmol) at −78 °C was treated with $\mathrm{Bu^tC{\equiv}P}$ (0.07 g, 0.70 mmol). After stirring the mixture at 0 °C for 1.5 h, all volatile material was removed *in vacuo*. The residue was dissolved in light petroleum (*ca.* 10 $\mathrm{cm^3}$), and chromatographed (−30 °C) on a Florisil column (2 × 20 cm). Elution with $\mathrm{Et_2O}$–light petroleum (1:9) developed a fast-moving brown band having a yellow tail. The latter was shown by i.r. spectroscopy to contain the rearrangement product (**6a**), and should not be allowed to contaminate the major product contained in the brown eluate. Removal of solvent from the latter afforded brown *microcrystals* of $[\mathrm{MoFe}\{\mu\text{-}\mathrm{C(C_6H_4Me\text{-}4)PC(Bu^t)}\}(\mathrm{CO})_4(\mathrm{PMe_3})(\eta\text{-}\mathrm{C_5H_5})]$ (**5a**) (0.123 g). A ^{1}H n.m.r. spectrum showed that (**5a**) contained *ca.* 5% of (**6a**).

(*ii*) In a similar synthesis, a thf (20 $\mathrm{cm^3}$) solution of complex (**4a**) (0.10 g, 0.20 mmol) was treated with an excess of $\mathrm{Pr^iC{\equiv}P}$ (*ca.* 0.40 mmol) at −78 °C. The mixture was stirred at 0 °C for 10 min, and then all volatile material was removed *in vacuo*. The residue was dissolved in $\mathrm{Et_2O}$–$\mathrm{CH_2Cl_2}$ (10 $\mathrm{cm^3}$, 4:1) and chromatographed on Florisil at −20 °C. Elution with the same solvent mixture gave a brown fraction. Solvent was removed *in vacuo*, and the residue was washed with $\mathrm{Et_2O}$–light petroleum (1:9, 2 × 2 $\mathrm{cm^3}$) at −78 °C giving brown-red *microcrystals* of $[\mathrm{MoFe}\{\mu\text{-}\mathrm{C(C_6H_4Me\text{-}4)PC(Pr^i)}\}(\mathrm{CO})_4(\mathrm{PMe_3})(\eta\text{-}\mathrm{C_5H_5})]$ (**5b**) (0.09 g).

(*iii*) A thf (20 $\mathrm{cm^3}$) solution of complex (**4b**) (0.08 g, 0.13 mmol) was treated with $\mathrm{Bu^tC{\equiv}P}$ (0.05 g, 0.50 mmol) at −78 °C. After warming to room temperature, the mixture was stirred for 5 h, during which the colour changed slowly to brown. Volatile material was removed *in vacuo*, and the residue was dissolved in $\mathrm{CH_2Cl_2}$–light petroleum (5 $\mathrm{cm^3}$, 2:3) and chromatographed (−20 °C) on Kieselgel (2 × 20 cm column). Elution with the same solvent mixture gave a red-brown fraction, which after removal of volatile material yielded brown *microcrystals* of $[\mathrm{WFe}\{\mu\text{-}\mathrm{C(C_6H_4Me\text{-}4)PC(Bu^t)}\}(\mathrm{CO})_4(\mathrm{PMe_3})(\eta\text{-}\mathrm{C_5H_5})]$ (**5c**) (0.047 g). Further elution with $\mathrm{CH_2Cl_2}$–light petroleum (4:1) removed a trace of the starting material (**4b**), identified by i.r. spectroscopy.

Isomerisation Reactions.—(*i*) A sample of complex (**5a**) (0.18 g, 0.29 mmol) was dissolved in $\mathrm{CH_2Cl_2}$ (3 $\mathrm{cm^3}$), and hexane (*ca.* 10 $\mathrm{cm^3}$) was layered on top without mixing. After 5 d at room temperature, solvent was removed *in vacuo*. The residue was dissolved in $\mathrm{CH_2Cl_2}$–light petroleum (10 $\mathrm{cm^3}$, 2:3), and the solution was chromatographed (−20 °C) on Kieselgel (2 × 20 cm column). Elution with $\mathrm{CH_2Cl_2}$–light petroleum (2:3) gave a trace of the starting product (**5a**), identified by ^{31}P-{^{1}H} n.m.r. spectroscopy. Further elution with $\mathrm{CH_2Cl_2}$–light petroleum (3:2) removed an orange band. Evaporation of solvent *in vacuo* afforded orange-red *microcrystals* of $[\mathrm{MoFe}\{\mu\text{-}\mathrm{C(C_6H_4Me\text{-}4)C(Bu^t)P}\}(\mu\text{-}\mathrm{CO})(\mathrm{CO})_3(\mathrm{PMe_3})(\eta\text{-}\mathrm{C_5H_5})]$ (**6a**) (0.057 g).

(*ii*) Compound (**5b**) (0.073 g, 0.12 mmol) was refluxed in $\mathrm{Et_2O}$ (50 $\mathrm{cm^3}$) for 2 d. Solvent was removed *in vacuo*. The residue was dissolved in $\mathrm{CH_2Cl_2}$–light petroleum (5 $\mathrm{cm^3}$, 2:3) and the solution was chromatographed (−20 °C) on Kieselgel (2 × 20 cm column). Elution with the same solvent mixture gave a trace of the precursor (**5b**), identified by ^{31}P-{^{1}H} n.m.r. spectroscopy. Further elution with $\mathrm{CH_2Cl_2}$–light petroleum (3:2) gave an orange-red band. Removal of solvent *in vacuo* afforded orange-red *microcrystals* of $[\mathrm{MoFe}\{\mu\text{-}\mathrm{C(C_6H_4Me\text{-}4)C(Pr^i)P}\}(\mu\text{-}\mathrm{CO})(\mathrm{CO})_3(\mathrm{PMe_3})(\eta\text{-}\mathrm{C_5H_5})]$ (**6b**) (0.04 g). A ^{31}P-{^{1}H} n.m.r. spectrum revealed the presence of a trace of impurity having a peak at δ 29 p.p.m., which could not be separated.

Crystal Structure Determinations.—Crystals of complexes (**2a**) and (**6a**) grow at −20 °C as dark green prisms and red platelets from $\mathrm{CH_2Cl_2}$ and $\mathrm{CH_2Cl_2}$–light petroleum (1:5) solutions, respectively. Crystals of suitable dimensions [*ca.* 0.05 × 0.08 × 0.50 mm for (**2a**), and 0.19 × 0.18 × 0.25 mm for (**6a**)] were sealed under nitrogen in Lindemann glass capillaries. Diffracted intensities were recorded at 293 K on a Nicolet R3m/V four-circle diffractometer (θ—2θ scans). For compound (**2a**), of the 5 418 unique reflections ($3 \leqslant 2\theta \leqslant 50°$), 3 179 had $F \geqslant 4\sigma(F)$, and only these were used in the final refinement of the structure. Intensity data were corrected for Lorentz, polarisation, and *X*-ray absorption effects.[14] Similarly, for (**6a**), of the 11 067 data, 7 489 had $F \geqslant 2\sigma(F)$, and only these were used in the final refinement of the structure, with corrections as for (**2a**).

Table 6. Fractional atomic co-ordinates (× 10^4) for complex (**6a**) with estimated standard deviations in parentheses

Atom	*x*	*y*	*z*	Atom	*x*	*y*	*z*
Mo(1A)	1 900(1)	2 172(1)	9 279(1)	Mo(1B)	3 452(1)	2 326(1)	2 865(1)
Fe(1A)	3 006(1)	3 197(1)	8 270(1)	Fe(1B)	4 092(1)	1 776(1)	4 094(1)
P(1A)	983(1)	2 111(1)	8 125(1)	P(1B)	3 234(1)	3 386(1)	3 877(1)
P(2A)	3 661(1)	2 041(1)	7 576(1)	P(2B)	5 877(1)	2 807(1)	4 604(1)
O(30A)	2 414(4)	4 817(4)	7 304(2)	O(30B)	4 954(4)	−423(3)	4 111(2)
O(50A)	5 478(4)	4 570(3)	8 757(2)	O(50B)	2 745(4)	1 426(4)	5 221(2)
O(60A)	620(4)	−310(3)	8 781(2)	O(60B)	4 488(5)	4 967(3)	2 816(2)
O(80A)	4 489(3)	1 635(3)	9 050(2)	O(80B)	6 157(4)	1 915(4)	3 187(2)
C(10A)	1 846(4)	3 894(3)	8 782(2)	C(10B)	2 352(4)	1 314(4)	3 623(2)
C(11A)	2 198(4)	5 124(4)	9 018(2)	C(11B)	1 653(4)	87(4)	3 643(2)
C(12A)	3 120(4)	5 501(4)	9 519(2)	C(12B)	2 032(5)	−830(4)	3 358(2)
C(13A)	3 470(5)	6 670(4)	9 697(2)	C(13B)	1 461(6)	−1 972(4)	3 455(3)
C(14A)	2 956(5)	7 497(4)	9 367(2)	C(14B)	500(6)	−2 237(5)	3 844(3)
C(15A)	2 071(5)	7 136(4)	8 861(3)	C(15B)	126(5)	−1 340(5)	4 133(3)
C(16A)	1 691(5)	5 975(4)	8 686(2)	C(16B)	684(5)	−198(4)	4 040(2)
C(17A)	3 370(6)	8 760(4)	9 557(3)	C(17B)	−73(6)	−3 489(5)	3 950(3)
C(20A)	633(4)	3 211(4)	8 631(2)	C(20B)	1 892(4)	2 354(4)	3 558(2)
C(21A)	−703(4)	3 355(4)	8 739(2)	C(21B)	571(5)	2 620(5)	3 384(3)
C(22A)	−1 249(5)	3 910(5)	8 147(3)	C(22B)	46(6)	2 866(5)	4 010(3)
C(23A)	−749(5)	4 091(4)	9 325(2)	C(23B)	−360(5)	1 667(5)	2 998(3)
C(24A)	−1 551(5)	2 162(4)	8 801(3)	C(24B)	706(6)	3 739(5)	2 999(3)
C(30A)	2 648(5)	4 161(5)	7 676(2)	C(30B)	4 615(5)	432(5)	4 102(2)
C(40A)	3 123(6)	501(4)	7 642(3)	C(40B)	6 635(6)	4 114(5)	4 231(3)
C(41A)	5 341(5)	2 169(5)	7 566(3)	C(41B)	5 702(6)	3 352(5)	5 391(3)
C(42A)	3 162(6)	2 259(6)	6 746(2)	C(42B)	7 151(5)	2 037(5)	4 767(3)
C(50A)	4 512(5)	4 042(4)	8 564(2)	C(50B)	3 312(5)	1 578(5)	4 786(2)
C(60A)	1 064(4)	652(4)	8 902(2)	C(60B)	4 093(5)	4 003(5)	2 902(3)
C(70A)	1 874(5)	3 087(4)	10 255(2)	C(70B)	2 397(7)	975(5)	2 087(3)
C(71A)	948(5)	2 069(5)	10 236(2)	C(71B)	2 159(7)	2 034(6)	1 895(3)
C(72A)	1 573(5)	1 134(4)	10 222(2)	C(72B)	3 302(9)	2 735(6)	1 788(3)
C(73A)	2 855(5)	1 569(4)	10 226(2)	C(73B)	4 248(7)	2 105(8)	1 911(3)
C(74A)	3 053(5)	2 789(4)	10 246(2)	C(74B)	3 671(8)	998(7)	2 093(3)
C(80A)	3 542(5)	1 992(4)	8 966(2)	C(80B)	5 122(5)	2 054(5)	3 253(2)

Crystal data for (**2a**). $C_{28}H_{31}FeO_5PW{\cdot}0.5CH_2Cl_2$, M = 761.7, monoclinic, a = 9.806(2), b = 16.899(3), c = 18.608(5) Å, β = 95.99(2)°, U = 3 066(1) Å^3, Z = 4, D_c = 1.65 g cm^{-3}, F(000) 1 500, space group $P2_1/n$ (non-standard setting of $P2_1/c$, no. 14), Mo-K_α X-radiation (graphite monochromator), $\bar{\lambda}$ = 0.710 73 Å, μ(Mo-K_α) = 44.7 cm^{-1}.

Crystal data for (**6a**). $C_{25}H_{30}FeMoO_4P_2$, M = 608.2, triclinic, a = 10.831(4), b = 11.749(6), c = 21.038(6) Å, α = 90.21(3), β = 95.58(3), γ = 101.26(3)°, U = 2 613 Å^3, Z = 4, D_c = 1.55 g cm^{-3}, F(000) 1 168, space group $P\bar{1}$, μ(Mo-K_α) = 11.7 cm^{-1}.

The structures were solved, and all non-hydrogen atoms located, by conventional heavy-atom and Fourier difference methods. Refinements were performed by full-matrix least squares on a digital μ-Vax computer. The carbon atom C(9) of the disordered solvent molecule in complex (**2a**) was refined isotropically, otherwise all the non-hydrogen atoms in both structures were refined anisotropically. There were two chemically identical but crystallographically independent molecules in the asymmetric unit of (**6a**). Hydrogen atoms were included at calculated positions (C–H 0.96 Å) with a common refined isotropic thermal parameter for the methyl hydrogen atoms and fixed isotropic thermal parameters (*ca.* 1.2 $U_{\text{equiv.}}$ of the parent carbon atom) for all other hydrogen atoms. The C_5Me_5, C_5H_5, and C_6H_4 rings were refined as rigid groups, C–C 1.395 Å. Refinements with weighting schemes w^{-1} = [$\sigma^2(F_o) + g|F_o|^2$] [with g = 001 10 for (**2a**) and 0.000 10 for (**6a**)] converged at R = 0.059 (R' = 0.055) for (**2a**) and R = 0.047 (R' = 0.038) for (**6a**). The final electron-density difference synthesis showed no residual peaks $\geqslant \pm$ 1.32 e Å^{-3} for (**2a**) and $\geqslant \pm$ 0.63 e Å^{-3} for (**6a**). Scattering factors and corrections for anomalous dispersion were taken from ref. 15. The atomic co-ordinates for (**2a**) and (**6a**) are listed in Tables 5 and 6, respectively.

Additional material available from the Cambridge Crystallographic Data Centre comprise H-atom co-ordinates, thermal parameters, and remaining bond lengths and angles.

Acknowledgements

We thank the S.E.R.C. for support and the Deutsche Forschungsgemeinschaft for a Fellowship (to J. S.).

References

1 Part 95, S. J. Davies, J. A. K. Howard, M. U. Pilotti, and F. G. A. Stone, *J. Chem. Soc., Dalton Trans.*, 1989, 2289.
2 J. C. Jeffery and M. J. Went, *Polyhedron*, 1988, **7**, 775.
3 (*a*) J. C. Jeffery, K. A. Mead, H. Razay, F. G. A. Stone, M. J. Went, and P. Woodward, *J. Chem. Soc., Dalton Trans.*, 1984, 1383; (*b*) M. Green, J. A. K. Howard, S. J. Porter, F. G. A. Stone, and D. C. Tyler, *ibid.*, p. 2553; (c) J. Hein, J. C. Jeffery, P. Sherwood, and F. G. A. Stone, *ibid.*, 1987, 2211; (*d*) E. Delgado, M. E. Garcia, J. C. Jeffery, P. Sherwood, and F. G. A. Stone, *ibid.*, 1988, 207; (*e*) H. E. Garcia, J. C. Jeffery, P. Sherwood, and F. G. A. Stone, *ibid.*, pp. 2431, 2443.
4 J. F. Nixon, *Chem. Rev.*, 1988, **88**, 1327.
5 M. Regitz and P. Binger, *Angew. Chem., Int. Ed. Engl.*, 1988, **27**, 1484.
6 A. F. Hill, J. A. K. Howard, T. P. Spaniol, F. G. A. Stone, and J. Szameitat, *Angew. Chem., Int. Ed. Engl.*, 1989, **28**, 210.
7 E. Delgado, J. Hein, J. C. Jeffery, A. L. Ratermann, F. G. A. Stone, and L. J. Farrugia, *J. Chem. Soc., Dalton Trans.*, 1987, 1191.
8 R. Hoffmann, *Angew. Chem., Int. Ed. Engl.*, 1982, **21**, 711.

9 M. E. Garcia, J. C. Jeffery, P. Sherwood, and F. G. A. Stone, *J. Chem. Soc., Dalton Trans.*, 1987, 1209.

10 P. G. Byrne, M. E. Garcia, N. H. Tran-Huy, J. C. Jeffery, and F. G. A. Stone, *J. Chem. Soc., Dalton Trans.*, 1987, 1243.

11 M. Green, J. A. K. Howard, A. P. James, A. N. de M. Jelfs, C. M. Nunn, and F. G. A. Stone, *J. Chem. Soc., Dalton Trans.*, 1986, 1697.

12 G. Becker, G. Gresser, and W. Uhl, *Z. Naturforsch., Teil B.*, 1981, **36**, 16.

13 W. Roesch, U. Vogelbacher, T. Allspach, and M. Regitz, *J. Organomet. Chem.*, 1986, **306**, 39.

14 G. M. Sheldrick, SHELXTL programs for use with the Nicolet–Siemens *X*-ray system, Göttingen, Revision 5, 1987.

15 'International Tables for *X*-Ray Crystallography,' Kynoch Press, Birmingham, 1974, vol. 4.

Received 25th April 1989; *Paper* 9/01715A